

# Utilization of Chondroitin Sulfate as an Anhydrous Proton Conductor

Masanori Yamada\* and Shunta Kawamura

Department of Chemistry, Faculty of Science, Okayama University of Science, Ridaicho, Kita-ku, Okayama 700-0005, Japan

\*E-mail: [myamada@chem.ous.ac.jp](mailto:myamada@chem.ous.ac.jp)

Received: 28 July 2018 / Accepted: 20 September 2018 / Published: 5 November 2018

---

Chondroitin sulfate C (CSC), one of the natural polysaccharides, is present in the connective tissue, brain, and cartilage. Therefore, the utilization of CSC has been limited to biological materials. In this study, we applied the CSC to the engineering field as a proton conducting material. The anhydrous proton conductive CSC-heterocycle composites were prepared by mixing the CSC material and the heterocycle imidazole (Im). The CSC-Im composite formed an acid-base composite by the electrostatic interaction between the acidic group, such as the carboxyl and sulfonic acid groups, and the non-protonated  $-N=$  of the Im molecule and showed a thermal stability at  $< 200$  °C. Additionally, the anhydrous proton conductivity of the CSC-Im composite increased with the addition of the Im molecule and indicated the maximum value of  $1.1 \times 10^{-3}$  S  $cm^{-1}$  at 130 °C under flowing dry-nitrogen. Furthermore, the activation energy ( $E_a$ ) of the proton conduction was 0.3 – 0.4 eV and this  $E_a$  value coincided with that of other anhydrous proton conductors. Therefore, the CSC-Im composite might be used as a novel anhydrous proton conductor.

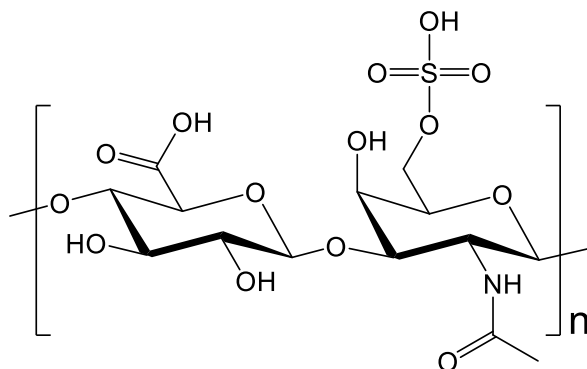
---

**Keywords:** Chondroitin sulfate, Acid-base composite, Anhydrous proton conductor, Biopolymer, Polymer electrolyte

## 1. INTRODUCTION

Chondroitin sulfate, a sulfated glycosaminoglycan composed of a chain of alternating sugars, *N*-acetylgalactosamine and glucuronic acid, is present in the connective tissue, brain, and cartilage [1,2]. Especially, chondroitin sulfate C (CSC) is one of the most popular chondroitins and found in animal cartilage. Scheme 1 shows the molecular structure of CSC. The CSC possesses carboxyl and sulfate groups in its molecular structure and behaves as an anionic biopolymer. The CSC forms the extracellular matrix with a three-dimensional network in our body and plays an important role in the cushion effect of cartilage [1,2]. Therefore, the CSC has been utilized as a biomedical, tissue

engineering, bioadhesive, and biocompatible materials [3-5]. However, the utilization of CSC has been demonstrated only from the viewpoint of biological science and the development of CSC based on its chemical and physical properties has not been reported to the best of our knowledge. Therefore, we demonstrated the novel utilization of CSC as an engineering and energy material, such as a proton conducting material.



**Scheme 1.** Molecular structure of chondroitin sulfate C (CSC).

The proton conducting material [6-8] is important for an actuator, an ion selective electrode, an electrolyte, a sensor materials, *etc.* Especially, anhydrous proton conducting materials has attracted the attention as novel electrolytes which are components in the operation of a polymer electrolyte fuel cell (PEFC) at intermediate temperatures (100 - 200 °C) [9-12]. This operation of the PEFC at intermediate temperatures has many advantages, such as improved CO tolerance of the Pt electrode, the higher energy efficiency, fuel management, simplified reforming/cooling units, and co-generation [9-12]. However, since the proton conducting mechanism of the practical electrolyte, such as the perfluorinated sulfonic acid membrane Nafion<sup>®</sup>, is based on the presence of the mobile water contents, such as  $\text{H}_3\text{O}^+$  or  $\text{H}_5\text{O}_2^+$ , in the humidified membrane, the proton conductivity above the boiling point of water (>100 °C) abruptly decreases due to the evaporation of the water from the membrane [12-14]. Therefore, the anhydrous proton conducting material is one of the important components for the operation of the PEFC at > 100 °C. Currently, the acid-base composites [15], the metal-organic frameworks (MOF) [16], the ionic liquids (IL) [17], *etc.*, have been reported for use as an anhydrous proton conducting material. However, although the MOF and the IL show a highly proton conductivity under low humidity or anhydrous conditions, these materials are difficult to form as membranes. The acid-base composites are prepared by mixing acidic and basic molecules (or polymers) and can easily form a membrane. In this case, the acidic and basic molecules behave as a proton donor and acceptor, respectively, and these behaviors also occur under low humidity or anhydrous conditions. Therefore, we became interested in the use to CSC as an anhydrous proton conductor. Since the CSC is an acidic biopolymer with the carboxyl and sulfate groups and these functional groups are regularly arranged in a polymer chain, these acidic groups play a role in the formation of the anhydrous proton conducting pathway. In addition, the CSC is easily obtained from cartilage which is discarded at food processing

plants. Therefore, the cost of utilizing of CSC as a proton conductor is lower than that of the artificial polymer.

In this study, we prepared a CSC-heterocycle composite by mixing CSC and a heterocycle, such as imidazole (Im). Since the CSC-Im composite material formed the acid-base composite by an electrostatic interaction between the acidic group of the CSC material and the basic group of the Im molecule, these materials showed a thermal stability at  $< 200^{\circ}\text{C}$ . Additionally, the proton conductivity of the CSC-Im composite increased with the addition of the Im molecule and showed the maximum proton conductivity of  $1.1 \times 10^{-3} \text{ S cm}^{-1}$  at  $130^{\circ}\text{C}$  under anhydrous conditions. The activation energy of the proton conduction was  $0.3 - 0.4 \text{ eV}$  and the proton conducting mechanism of the CSC-Im composite was based on an anhydrous proton conducting mechanism with an intermolecular proton transfer.

## 2. EXPERIMENTAL SECTIONS

### 2.1. Material

The chondroitin sulfate C sodium salt and imidazole were purchased from Wako Pure Chemical Industries, Ltd., Osaka, Japan. The ion exchange resin, Amberlite IR 120(H), was obtained from Supelco, Inc., Bellefonte, PA, USA. Solvents of analytical grade were used in all the experiments. Ultrapure water (Merck KGaA, Darmstadt, Germany) was used in this research.

### 2.2. Preparation of the CSC-Im composite

The chondroitin sulfate C sodium salt was changed from the  $\text{Na}^+$  form to  $\text{H}^+$  form by the Amberlite IR 120(H) ion exchange resin [18]. The ion exchange of the CSC material was confirmed by a pH measurement. The amount of acidic groups, such as the carboxyl and sulfonic acid groups, in the CSC material was estimated by the neutralization titration and this value was  $4.71 \times 10^{-3} \text{ mol g}^{-1}$ . The CSC material and Im molecule were mixed in a molar ratio. The CSC-Im composite was prepared as follows: the Im molecule was dissolved in the aqueous CSC solution ( $50 \text{ mg ml}^{-1}$ ). The molar ratio of the Im molecule was 10 – 95 mol%. The mixed solution was incubated at room temperature for 24 hours, 100  $\mu\text{l}$  cast on a Teflon<sup>®</sup> plate, dried at room temperature for 48 hours, then heated at  $120^{\circ}\text{C}$  for 1 hour. The obtained brown CSC-Im composite film was used in the experiments.

### 2.3. Characterization of the CSC-Im composite

The thermal stabilities of the CSC-Im composite were analyzed using a DTG-60 thermogravimetric (TG) - differential thermal analyzer (DTA) (Shimadzu Corp., Kyoto, Japan). The TG-DTA measurement was carried out at the heating rate of  $10^{\circ}\text{C min}^{-1}$  from room temperature to  $160^{\circ}\text{C}$  under flowing dry-nitrogen. Sample weights of the TG-DTA measurements were normalized at 1 mg. The infrared (IR) absorption spectra of the CSC-Im composite were measured by the attenuated

total reflection (ATR) method with a diamond prism using an FT-IR 8400 Fourier transform infrared spectrometer (Shimadzu Corp.). The IR spectrum was measured with the resolution of  $4\text{ cm}^{-1}$ .

#### 2.4. Proton conductive measurement of CSC-Im composite

The proton conductivity of the CSC-Im composite was demonstrated by the a.c. impedance method in the frequency range from 4 Hz to 1 MHz using a chemical impedance analyzer 35320-80 (Hioki Co., Nagano, Japan) in a stainless steel vessel from room temperature to  $160\text{ }^{\circ}\text{C}$  under flowing dry-nitrogen [18,19]. The CSC-Im composite was sandwiched between two Pt electrodes (diameter: 6 mm) with the Teflon<sup>®</sup> spacer [19,20]. The direction of the conductive measurement was perpendicular to the composite. Before the measurements of the proton conductions, the composites were dried at  $160\text{ }^{\circ}\text{C}$  for 2 hours in a stainless steel vessel to evaporate the water and volatile components from the composite. The conductivities of the composite materials were determined from a typical impedance response (Cole-Cole plots).

### 3. RESULTS AND DISCUSSION

#### 3.1. Thermal stability of CSC-Im composite

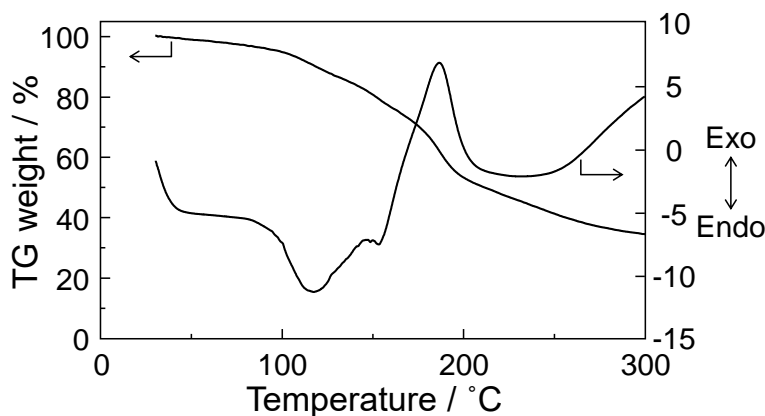


**Figure 1.** TG and DTA curves of CSC material without any heat treatment. These measurements were done at the heating rate of  $10\text{ }^{\circ}\text{C min}^{-1}$  under flowing dry-nitrogen. Triplicate experiments gave similar results.

The thermal stability of the CSC material without the thermal treatment, such as heating at  $120\text{ }^{\circ}\text{C}$  for 1 hour, was analyzed by the TG-DTA. Figure 1 shows the TG and DTA of the CSC material without the thermal treatment. The non-treated CSC material showed the TG weight loss of approximately 50% at  $< 200\text{ }^{\circ}\text{C}$ . Additionally, the CSC material showed a large endothermic peak at  $98.3\text{ }^{\circ}\text{C}$ . As a result, the TG weight loss of the CSC material at  $< 200\text{ }^{\circ}\text{C}$  is mainly due to the

evaporation of water from the CSC material. Therefore, the CSC materials were treated by heating at 120 °C for 1 hour to evaporate the water content from the material.

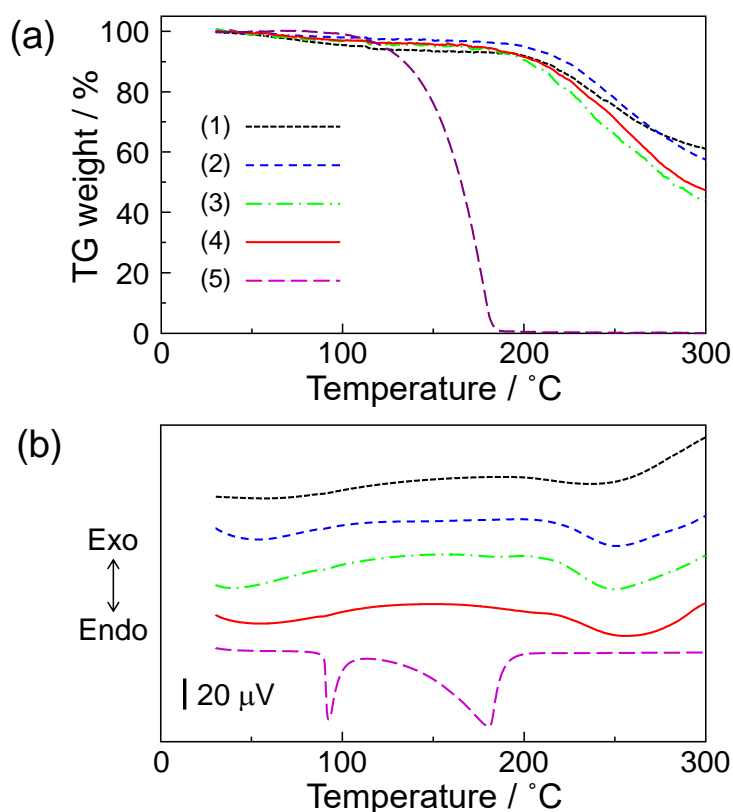


**Figure 2.** TG (a) and DTA (b) curves of (1) CSC material without the composite, (2) CSC-30 mol% Im composite, (3) CSC-50 mol% Im composite, (4) CSC-90 mol% Im composite, and (5) Im molecule without the composite. Triplicate experiments gave similar results.

The CSC-Im composites were prepared by mixing the CSC material and Im molecule. These composites were heated at 120 °C for 1 hour to evaporate the water in the composite. The CSC-Im composites were analyzed by TG-DTA. Figures 2 (a) and (b) show the TG and DTA of (1) the CSC material without the composite, (2) CSC-30 mol% Im composite, (3) CSC-50 mol% Im composite, (4) CSC-90 mol% Im composite, and (5) Im molecule without the composite. The CSC material without the composite had a TG weight loss of approximately 5% at < 200 °C. The DTA curve showed a small endothermic peak at < 200 °C. Therefore, the TG weight loss of the CSC material at < 200 °C is due to evaporation of the water from the material. In contrast, the Im material without the composite showed endothermic peaks at 88.0 °C and 135.2 °C, related to the melting and boiling of the Im molecule, respectively (line (5) in Figure 2) [19]. These endothermic peaks of the Im molecule disappeared in the CSC-Im composite materials. Similar phenomena have been reported for the chitin phosphate-heterocyclic molecule composite [21], double-stranded DNA-Im composite [18], and ligninsulfonic acid-Im composite materials [22]. These results suggested that the CSC material and Im molecules are thermally stabilized by mixing the Im molecule and CSC.

On the other hand, at 300 °C, the TG weight loss of the CSC-Im composite was > 40%. In addition, the composite showed a large endothermic peak attributed to the thermal decomposition at > 200 °C. These results suggested that the CSC-Im material cannot use at > 200 °C.

### 3.2. Molecular structure of the CSC-Im composite

The molecular structures of the CSC-Im composite were analyzed by an IR spectrometer equipped with a diamond ATR prism. Figure 3 shows the IR spectra of (a) CSC material without the composite, (b) CSC-10 mol% Im composite, (c) CSC-30 mol% Im composite, (d) CSC-50 mol% Im composite, (e) CSC-70 mol% Im composite, (f) CSC-90 mol% Im composite, and (g) Im molecule without the composite. The CSC material without the composite showed absorption bands at 1734  $\text{cm}^{-1}$  and 1217  $\text{cm}^{-1}$ , related to the stretching vibration of C=O in the  $-\text{COOH}$  group [23] and the stretching vibration of S=O in  $-\text{OSO}_3\text{H}$  [23-25], respectively. When the Im molecule was added to the CSC, the absorption band at 1734  $\text{cm}^{-1}$  relatively decreased and disappeared at > 70 mol% Im. In addition, the absorption bands at 1600  $\text{cm}^{-1}$  and 1400  $\text{cm}^{-1}$ , attributed to the symmetric and asymmetric stretching vibrations of the deprotonated  $-\text{COO}^-$  [23], respectively, relatively increased. Furthermore, although the absorption band at 1217  $\text{cm}^{-1}$  relatively decreased with the addition of the Im molecules, the absorption band at 1000  $\text{cm}^{-1}$ , related to the formation of sulfonic acid salts [26], increased. These results suggested that the  $-\text{COOH}$  and  $-\text{OSO}_3\text{H}$  groups in the CSC material form the deprotonated groups, such as the  $-\text{COO}^-$  and  $-\text{OSO}_3^-$  groups, respectively, by the addition to Im molecules and produce the free proton.

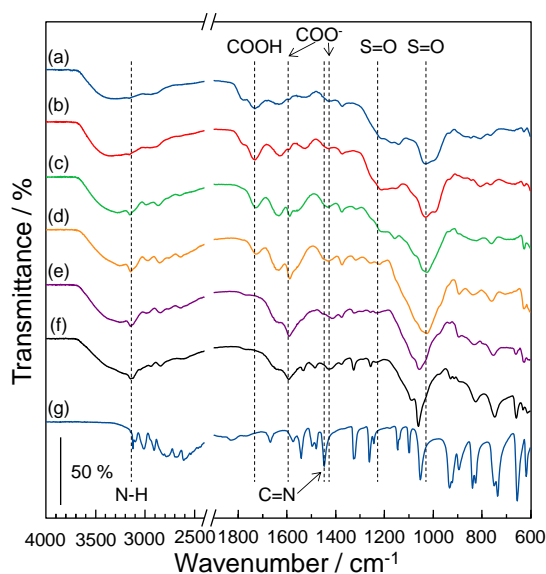


**Figure 3.** IR spectra of (a) CSC material without the composite, (b) CSC-10 mol% Im composite, (c) CSC-30 mol% Im composite, (d) CSC-50 mol% Im composite, (e) CSC-70 mol% Im composite, (f) CSC-90 mol% Im composite, and (g) Im molecule without the composite. The IR spectrum was measured at the resolution of 4  $\text{cm}^{-1}$ . Triplicate experiments gave similar results.

The Im molecule without the composite showed an absorption band at  $3100\text{ cm}^{-1}$ , which corresponded to the stretching band of the N-H group [23,27]. When the Im molecules were added to the CSC material, this adsorption band at  $3100\text{ cm}^{-1}$  relatively increased. Additionally, the absorption band at  $1448\text{ cm}^{-1}$ , attributed to the aromatic C=N of the Im molecule [23], relatively decreased with the addition to the CSC material. These phenomena were related to the formation of the N-H part and deforming of the aromatic C=N group by the addition to the CSC material.

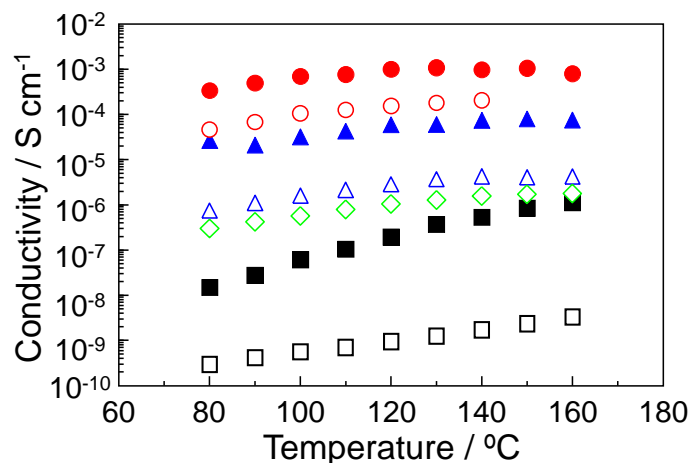
These phenomena are considered as follows: the acidic group, such as the  $-\text{COOH}$  and  $-\text{OSO}_3\text{H}$  groups, in the CSC material deprotonated by the addition to the basic Im molecule and formed the negatively charged acidic group, such as the  $-\text{COO}^-$  and  $-\text{OSO}_3^-$  groups. In contrast, the non-protonated  $-\text{N}=\text{}$  groups in the basic Im molecule interacted with the free proton from the CSC material and formed the N-H group. Therefore, the CSC-Im composite produced the acid-base salts, such as the imidazolium organic salts, through the electrostatic interaction between the acidic group, such as the carboxyl and sulfonic acid groups, and non-protonated  $-\text{N}=\text{}$  of the Im molecule. The formation of the acid-base salts induced the thermal stabilization of the CSC-Im composite. Similar phenomena, such as the thermal stabilization by the acid-base interaction, have been reported for the chitin phosphate-heterocyclic molecule composite [21], double-stranded DNA-Im composite [18], and ligninsulfonic acid-Im composite materials [22].

### 3.3. Anhydrous proton conduction of the CSC-Im composite

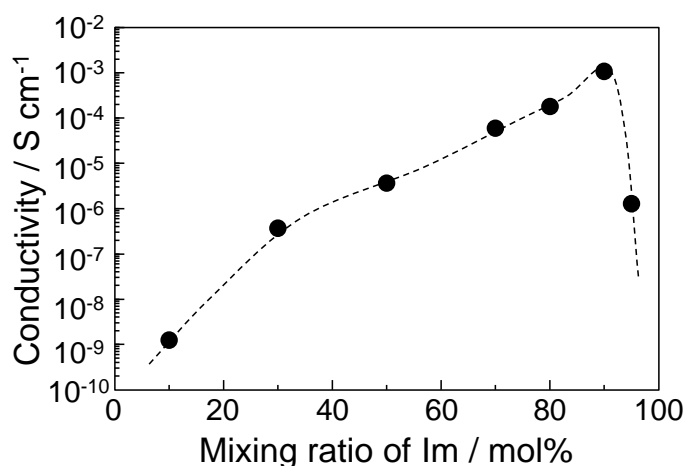
The proton conductive measurements of the CSC-Im composite were done by the a.c. impedance method over the frequency range from 4 Hz to 1 MHz under flowing dry-nitrogen. The thickness of the CSC-Im composite sample was ca.  $150\text{ }\mu\text{m}$ . The features of the Cole-Cole plots for the CSC-Im composite are similar to that of highly proton conducting materials [13]. The resistances of the composites were obtained from the extrapolation to the real axis and the proton conductivities of material were calculated from the resistance, the thickness of the composite, and the surface area of the Pt electrode. Additionally, according to the TG-DTA measurements, no diffusible ions other than the protons existed in these materials at  $< 200\text{ }^\circ\text{C}$  (see Figure 2). Furthermore, the proton conducting samples in a stainless steel vessel were heated at  $160\text{ }^\circ\text{C}$  for 2 hours under flowing dry-nitrogen before the measurement. Therefore, the impedance responses of the CSC-Im composites are based on the anhydrous proton transfer without the assistance of diffusible vehicle molecules, such as water molecules [15].

Figure 4 shows the proton conduction of ( $\square$ ) CSC-10 mol% Im composite, ( $\blacksquare$ ) CSC-30 mol% Im composite, ( $\triangle$ ) CSC-50 mol% Im composite, ( $\blacktriangle$ ) CSC-70 mol% Im composite, ( $\circ$ ) CSC-80 mol% Im composite, ( $\bullet$ ) CSC-90 mol% Im composite, and ( $\diamond$ ) CSC-95 mol% composite. The proton conductions of the CSC-Im composite material increased with the temperature and reached a maximum value at  $130 - 140\text{ }^\circ\text{C}$ . At  $> 140\text{ }^\circ\text{C}$ , the proton conductions slightly decreased. This phenomenon is due to the thermal decomposition of the CSC, since the DTA curve of the CSC material without the thermal treatment shows a small endothermic peak at  $145.8^\circ\text{C}$  related to the thermal decomposition. Figure 5 shows the change in the proton conduction at  $130\text{ }^\circ\text{C}$  as a function of

the Im molecule mixing ratio from 10 to 95 mol%. The proton conduction increased with the addition of the Im molecule and reached a maximum value at 90 mol%. The maximum proton conductivity was  $1.1 \times 10^{-3} \text{ S cm}^{-1}$ . In contrast, the CSC material without the composite did not show any measurable proton conductivity ( $< 10^{-10} \text{ S cm}^{-1}$ ). Additionally, the Im molecule without the composite did not indicate a proton conduction due to their melting and evaporation during the heat treatment process at  $160^\circ\text{C}$  for 2 hours.



**Figure 4.** Proton conductivities of CSC-Im composite under dry-nitrogen flow. (□) CSC-10 mol% Im composite, (■) CSC-30 mol% Im composite, (△) CSC-50 mol% Im composite, (▲) CSC-70 mol% Im composite, (○) CSC-80 mol% Im composite, (●) CSC-90 mol% Im composite, and (◇) CSC-95 mol% composite. The proton conductivity measurement was performed by the a.c. impedance method. These samples were dried at  $160^\circ\text{C}$  for 2 hours under flowing dry-nitrogen.



**Figure 5.** Change in the proton conduction at  $130^\circ\text{C}$  as a function of the Im mixing ratio from 10 to 95 mol%. The proton conductive measurements were done under flowing dry-nitrogen.



Finally, we determined the activation energy ( $E_a$ ) of the proton conduction for the CSC-Im composite. Figure 6 shows the Arrhenius plots of the proton conduction of ( $\square$ ) CSC-10 mol% Im composite, ( $\blacksquare$ ) CSC-30 mol% Im composite, ( $\triangle$ ) CSC-50 mol% Im composite, ( $\blacktriangle$ ) CSC-70 mol% Im composite, ( $\circ$ ) CSC-80 mol% Im composite, ( $\bullet$ ) CSC-90 mol% Im composite, and ( $\diamond$ ) CSC-95 mol% composite in the region of 80 °C to 130 °C. The solid lines in Figure 6 are the results of the least-squares fitting. The Arrhenius plots showed a linear relationship in the region of 80 °C to 130 °C. Therefore, in these regions, the proton conduction of the CSC-Im composite is related to a single proton conductive mechanism. The  $E_a$  of the proton conduction was calculated from the slope of the line. Table 1 shows the  $E_a$  values of the proton conduction in the CSC-Im composite. Although the  $E_a$  indicated the highest value at 30 mol% Im, the other values showed a constant value of 0.2 – 0.4 eV. These  $E_a$  values, such as 0.2 – 0.4 eV, are one order higher than that of the fully swelled Nafion<sup>®</sup> membrane [13,14]. These results suggested that the proton conduction of the CSC-Im composite is based on the anhydrous proton conducting mechanism without the assistance of diffusible water molecules. In fact, similar  $E_a$  values have been reported for various anhydrous proton conductors [15,22,28-30].

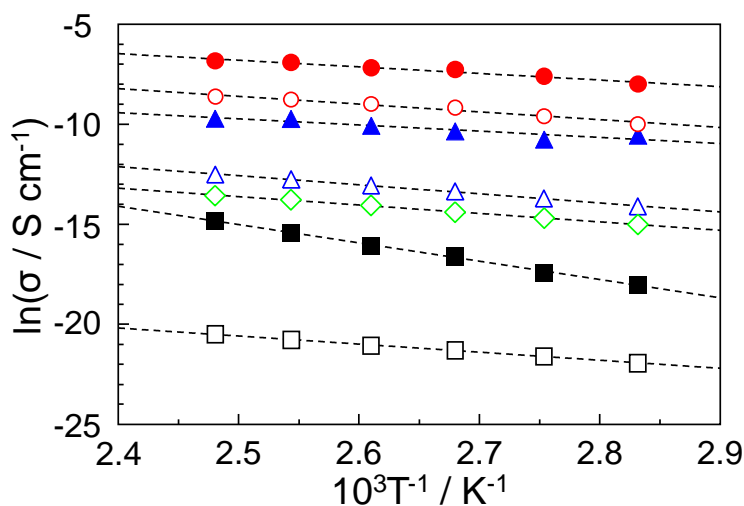


**Figure 6.** Arrhenius plots of the proton conductivity of the CSC-Im composite. The solid lines are the results of a least-squares fitting. ( $\square$ ) CSC-10 mol% Im composite, ( $\blacksquare$ ) CSC-30 mol% Im composite, ( $\triangle$ ) CSC-50 mol% Im composite, ( $\blacktriangle$ ) CSC-70 mol% Im composite, ( $\circ$ ) CSC-80 mol% Im composite, ( $\bullet$ ) CSC-90 mol% Im composite, and ( $\diamond$ ) CSC-95 mol% composite.

**Table 1.** The activation energy ( $E_a$ ) of proton conduction in the CSC-Im composite.

CSC-Im composite	$E_a$ / eV
CSC-10 mol% Im	0.35
CSC-30 mol% Im	0.79
CSC-50 mol% Im	0.39
CSC-70 mol% Im	0.26
CSC-80 mol% Im	0.33
CSC-90 mol% Im	0.28
CSC-95 mol% Im	0.36

**Table 2.** Anhydrous proton conductivity and its activation energy ( $E_a$ ) of various acid-base composite materials with the imidazole molecules.

Composite materials	Anhydrous proton conductivity	$E_a$	Ref.*
Poly(vinylphosphonic acid)-imidazole	$7 \times 10^{-3} \text{ S cm}^{-1}$ (at 150 °C)	0.2 – 0.4 eV	15,19
Chitin phosphate-imidazole	$7 \times 10^{-3} \text{ S cm}^{-1}$ (at 150 °C)	0.4 eV	15,21
Alginic acid-imidazole	$2 \times 10^{-3} \text{ S cm}^{-1}$ (at 130 °C)	0.2 – 0.4 eV	15
DNA-imidazole	$5.2 \times 10^{-3} \text{ S cm}^{-1}$ (at 160 °C)	0.3 – 1.8 eV	18
Ligninsulfonic acid-imidazole	$9.1 \times 10^{-4} \text{ S cm}^{-1}$ (at 130 °C)	0.2 – 1.4 eV	22
Polyacrylic acid-imidazole	$1 \times 10^{-3} \text{ S cm}^{-1}$ (at 120 °C)	–	31,32
Poly(2-acrylamido-2-methyl-1-propanesulfonic acid)-imidazole	$1.45 \times 10^{-3} \text{ S cm}^{-1}$ (at 100 °C)	–	31,33
Chondroitin sulfate C-imidazole	$1.1 \times 10^{-3} \text{ S cm}^{-1}$ (at 130 °C)	0.2 – 0.8 eV	This work

\*Reference number

Table 2 shows the anhydrous proton conductivity and its  $E_a$  of various acid-base composite materials with the Im molecules. These composite materials with the Im molecules showed the anhydrous proton conductivity on the order of  $10^{-4} - 10^{-3} \text{ S cm}^{-1}$  at the intermediated temperature (100 – 200 °C). Additionally, the  $E_a$  of proton conduction was largely changed by the mixing ratio of Im molecules. Generally, the proton conducting mechanism of the acid-base composite material with the Im molecules was based on the proton transfer between the Im molecules [14]. In this case, the proton transfer occurs from protonated Im molecules to non-protonated neighboring Im molecules and the  $E_a$  of the proton conduction between the Im molecules is 0.2 – 0.4 eV [15,18,19,22]. In our investigation, the proton transfer of the CSC-Im composite can be explained by a similar proton conducting mechanism. At a low mixing ratio of Im ( $\leq 50 \text{ mol}\%$ ), since the distance between the Im molecules was too long to transfer the proton, the composite showed a low proton conductivity. Consequently, the  $E_a$  of the proton conduction showed a high value ( $> 0.35 \text{ eV}$ ). At the high mixing ratio of Im ( $\geq 70 \text{ mol}\%$ ), since the Im molecules form the proton conducting pathway in the CSC-Im composite, the proton in the composite easily transferred from the protonated Im molecules to the non-protonated neighboring Im molecules with the low  $E_a$  ( $< 0.35 \text{ eV}$ ). Similar phenomena, such as the change of proton conducting mechanism by the mixing ratio of Im, have been reported for double-stranded DNA-Im [18] and ligninsulfonic acid-Im composite material [22]. As a result, the CSC-Im composite showed a highly anhydrous proton conductivity on the order of  $10^{-3} \text{ S cm}^{-1}$  at 130 °C. In contrast, at  $\geq 95 \text{ mol}\%$  Im, since the ratio of the non-protonated Im molecule decreased in the CSC-Im composite, the proton conduction abruptly decreased.

#### 4. CONCLUSION

We prepared the CSC-Im composite by mixing chondroitin sulfate C (CSC) and the heterocycle imidazole (Im) molecule. The CSC-Im composite formed an acid-base composite by the electrostatic interaction between the acidic group, such as the carboxyl and sulfonic acid groups, and the non-protonated  $-N=$  of Im molecule. As a result, The CSC-Im composite showed a thermal stability at  $< 200$  °C. In addition, the anhydrous proton conductivity of the CSC-Im composite increased with the addition of the Im molecules and showed a maximum value of  $1.1 \times 10^{-3}$  S  $\text{cm}^{-1}$  at 130 °C under flowing dry-nitrogen. Furthermore, the activation energy ( $E_a$ ) of the maximum proton conduction was 0.3 – 0.4 eV. This  $E_a$  value was similar to that of other reported anhydrous proton conductors. Therefore, the anhydrous proton conductive CSC-Im composite may have the potential not only as an electrolyte of PEFCs, but also for various applications in an implantable battery and biosensor, *etc.*

#### References

1. B. Alberts, A. Johnson, J. Lewis, D. Morgan, M. Raff, K. Roberts, P. Walter, Molecular biology of the cell, Garland Science, New York, 2014.
2. C. Schiraldi, D. Cimini, M.D. Rosa, *Appl. Microbiol. Biotechnol.*, 87 (2010) 1209.
3. A. Köwitsch, G. Zhou, T. Groth, *J. Tissue Eng. Regen. Med.*, 12 (2018) 23.
4. X. Yang, W. Liu, N. Li, M. Wang, B. Liang, I. Ullah, A.L. Neve, Y. Feng, H. Chen, C. Shi, *Biomater. Sci.*, 5 (2017) 2357.
5. S. Bhowmick, A.V. Thanusha, A. Kumar, D. Scharnweber, S. Rother, V. Koul, *RSC Adv.*, 8 (2018) 16420.
6. H. Gao, K. Lian, *RSC Adv.*, 4 (2014) 33091.
7. L. Cao, X. He, Z. Jiang, X. Li, Y. Li, Y. Ren, L. Yang, H. Wu, *Chem. Soc. Rev.*, 46 (2017) 6725.
8. K.D. Kreuer, *Chem. Mater.*, 26 (2014) 361.
9. M. Rikukawa, K. Sanui, *Prog. Polym. Sci.*, 25 (2000) 1463.
10. J.A. Asensio, E.M. Sánchez, P. Gómez-Romero, *Chem. Soc. Rev.*, 39 (2010) 3210.
11. J. Peron, Z. Shi, S. Holdcroft, *Energy Environ. Sci.*, 4 (2011) 1575.
12. A.C. Dupuis, *Prog. Mater. Sci.*, 56 (2011) 289.
13. Y. Sone, P. Ekdunge, D. Simonsson, *J. Electrochem. Soc.*, 143 (1996) 1254.
14. K.D. Kreuer, *Chem. Mater.*, 8 (1996) 610.
15. I. Honma, M. Yamada, *Bull. Chem. Soc. Jpn.*, 80 (2007) 2110.
16. S. Horike, D. Umeyama, S. Kitagawa, *Acc. Chem. Res.*, 46 (2013) 2376.
17. J. Sun, L.R. Jordan, M. Forsyth, D.R. MacFarlane, *Electrochim. Acta*, 46 (2001) 1703.
18. M. Yamada, A. Goto, *Polym. J.*, 44 (2012) 415.
19. M. Yamada, I. Honma, *Polymer*, 46 (2005) 2986.
20. M. Suzuki, T. Yoshida, S. Kobayashi, T. Koyama, Kimura, K. Hanabusa, H. Shirai, *Phys. Chem. Chem. Phys.*, 1 (1999) 2749.
21. M. Yamada, I. Honma, *Angew. Chem. Int. Ed.*, 43 (2004) 3688.
22. M. Yamada, M. Takeda, *Int. J. Electrochem. Sci.*, 13 (2018) 7291.
23. R.M. Silverstein, F.X. Webster, Spectrometric Identification of Organic Compounds, John Wiley & Sons, (1998) New York.
24. M. Tamaddon, R.S. Walton, D.D. Brand, J.T. Czernuszka, *J. Mater. Sci. Mater. Med.*, 24 (2013) 1153.
25. S.B. Etcheverry, P.A.M. Williams, E.J. Baran, *Biol. Trace Elem. Res.*, 42 (1994) 43.

26. S. Nakanishi, F. Yoshimura, *Kogyo Kagaku Zasshi*, 73 (1970) 323.
27. M. Kawahara, J. Morita, M. Rikukawa, K. Sanui, N. Ogata, *Electrochim. Acta*, 45 (2000) 1395.
28. H. Iwahara, *Solid State Ionics* 9 (1996) 86.
29. Y.M. Li, M. Hibino, M. Miyayania, T. Kudo, *Solid State Ionics* 134 (2000) 271.
30. P. Colomban, A. Novak, *J. Mol. Struct.*, 177 (1998) 277.
31. S.Ü. Çelik, A. Bozkurt, S.S. Hosseini, *Prog. Polym. Sci.*, 37 (2012) 1265.
32. A. Bozkurt, W.H. Meyer, G. Wegner, *J. Power Sources*, 123 (2003) 126.
33. H. Erdemi, A. Bozkurt, W.H. Meyer, *Synth. Met.*, 143 (2004) 133.

© 2018 The Authors. Published by ESG ([www.electrochemsci.org](http://www.electrochemsci.org)). This article is an open access article distributed under the terms and conditions of the Creative Commons Attribution license (<http://creativecommons.org/licenses/by/4.0/>).